The estimation of spray angles in a windshield wiper nozzle

Yudaya Sivathanu*[1], Jongmook Lim[1], Deepa Divakaran[1], and Marcus Wolverton[1]
[1]En'Urga Inc., West Lafayette, Indiana, USA
*Corresponding author email :sivathan@enurga.com

Abstract

The estimation of spray angles is crucial in several automotive, pharmaceutical, and aerospace industry applications. This study looks at spray angles that are used in windshield wipers. The spray is characterized by five angles: the aim angle, fan angle, roll angle, yaw angle, and thickness angle. The definitions of the common angles used in the characterization of windshield wipers are presented. An estimation of these angles from two windshield nozzles was obtained using an optical patternator. The optical patternator measures the extinction at six different view angles. The effect of radial and angular spatial resolution on the estimation of these spray angles is presented. It was determined that some of these angles are more sensitive to radial resolution and less sensitive to angular resolution. Therefore, a deconvolution method that provides varying angular and radial resolution after the measurements have been the key to the spray's characterization from a windshield wiper.

Keywords

Spray angles, extinction tomography, windshield wiper, flat spray

Introduction

Spray angle and spray inclination are essential in a variety of applications [1]. The spray angle and its pattern directly impact the amounts of pollution emitted from internal combustion engines since they determine the amount of wall wetting [2,3]. The spray angle and inclination are directly related to the quality and thickness of coating in plasma coating applications [4]. In painting applications, the spray inclination and angle determine the transfer efficiency [5]. The spray inclination and angle determine the heat transferred from flat and finned surfaces used in spray cooling applications [6]. In agricultural applications, spray angle is the critical parameter that determines the height of the boom and the number of nozzles required to achieve uniform coverage [7]. Although spray angle and inclination are essential in most applications, they are difficult to estimate.

The most commonly used method of estimating spray angles is mechanical, employing either collection cups in various shapes and sizes [8] or special paper [9]. These mechanical devices suffer from several systematic and random errors, primarily from stagnation effects [10]. Due to these errors, optical imaging was adopted for spray angle measurements. The earliest devices used white illumination and mechanical protractors [1]. These are, however, subject to operator interpretation. Tests have shown that the same operator can measure spray angles differently by more than 20% on different days [1]. The mechanical protractors have since been replaced with digital cameras.

Mie scattered light from a laser sheet [11] and conventional back-lit imaging [12] are the commonly used methods to obtain spray angles. In addition, laser-induced fluorescence [13] and digital holography [14] have also been used to obtain spray angles. All the above optical methods measure the surface area density of drops (scattering and back-lit illumination) or the mass concentrations (fluorescence). There is no flux information

available, unlike most mechanical patternators. Mie and fluorescence imaging typically work only for dilute sprays and require extensive corrections even for moderately dense sprays [15]. Therefore they are not ideally suited for quality audit purposes in dense sprays.

Conventional back-lit imaging (which is, in principle, an extinction measurement) is the most robust optical method for determining spray angles and has been recommended by SAE [16]. However, during a round-robin testing procedure [16], it was observed that the differences in spray angles reported by three independent labs could be as high as 66%. The primary reason cited for this difference was the variation in standard test protocols, which include variation in ambient lighting and determination of image threshold. In addition, recent numerical investigations have revealed that spray angles measured using complete flow field imaging suffer from multiple scattering effects, which are more significant in dense sprays [17]. Over the last two decades, spray angles in many industries are routinely measured using multiple view angle measurements of the extinction of a laser sheet oriented perpendicular to the spray [18,19]. The method is immune to ambient lighting and does not suffer from multiple scattering effects since only a thin laser sheet is used.

This article's primary objective was to explore the use of extinction tomography for angle measurements in sprays from windshield wipers based on the preceding discussion. In addition to the main spray angles, this article examines the common terminology used in the industry to characterize the inclination angles in flat fan sprays. Sample spray angle estimates obtained using extinction tomography from two nozzles are also presented.

Material and Methods

The SETscan optical patternator measures the path integrated extinction along six collimated beams as shown in Fig.1.
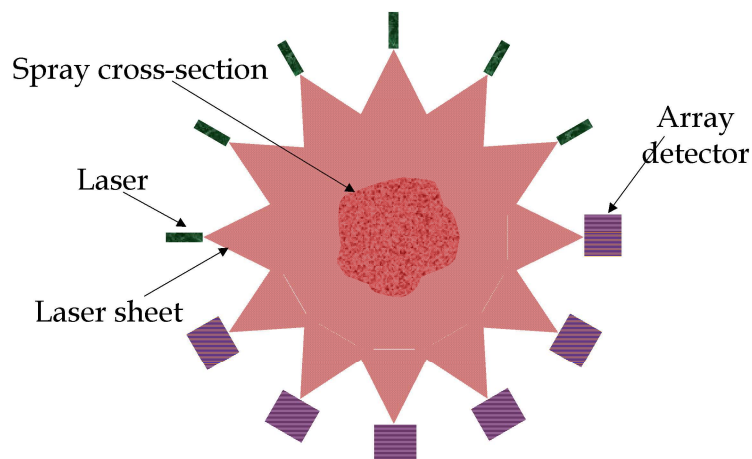

Figure 1. Schematic presentation of the optical patternator..

The path integrated extinction is deconvoluted using the Maximum Likelihood Estimation method [20] to provide the local drop surface area density. The drop surface area density is the product of the surface area of the drops and the number of drops per unit volume. The drop surface area densities are used to define all the spray angles discussed in this paper.

Two nozzles were used in this study. A photograph of the experimental arrangement is shown in Fig. 2. The nozzle is mounted on a linear traverse so that the nozzle exit can be positioned at a fixed distance from the measurement plane. All measurements were obtained at a distance of 50 mm below the exit of the nozzle.
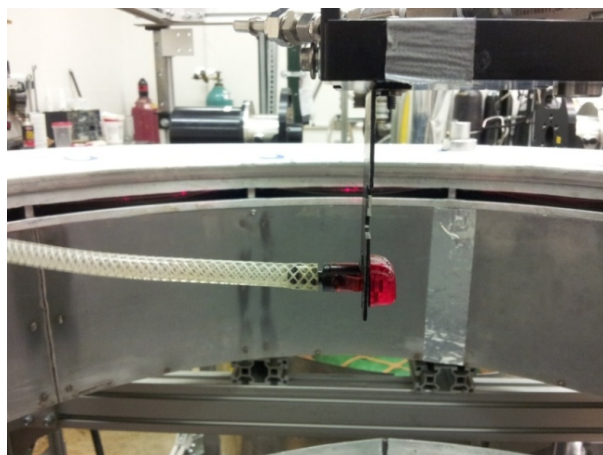
Figure 2. Experimental arrangement for the determination of spray angles in a windshield wiper.

The positioning accuracy of the nozzles to the centre of the patternator is about +/-1mm. The nozzles were connected to a reservoir maintained at 35 PSI using compressed air. The pressure drop from the reservoir to the nozzles due to the tubes' length is approximately 6 PSI. Therefore, the pressure at the back end of the nozzle is estimated to be close to 29 PSI. The measurements were obtained at 40 mm below the exit plane from the sample injector operating at 35 PSI. A stop valve was used to control the flow of the water to the nozzle. A reference voltage for the six arrays was first obtained on the patternator for 1 second. The flow to the nozzle was then started. Once the flow stabilized in a period of a few second, data was collected for 5 seconds. The angles reported by the patternator are validated using reference neutral density filters that provide a theoretical angle. The angle provided by the patternator is within 1% of this theoretical angle.

Results and Discussion

Data was collected from two nozzles, labelled A and B, for 5 seconds at 1,000 Hz. The mean absorptances measured at 35 PI for nozzle A are shown in Fig. 3.
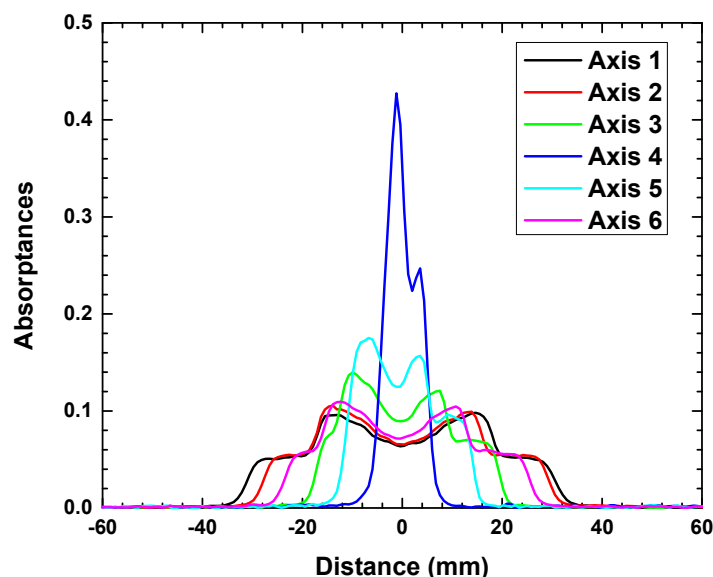

Figure 3. Mean absorptances for the windshield wiper nozzle A.

The mean extinction data were deconvoluted using the maximum likelihood estimation method [18] to provide the local surface area densities in the spray. The contour plot of surface area densities from Nozzle A is shown in Fig. 4.
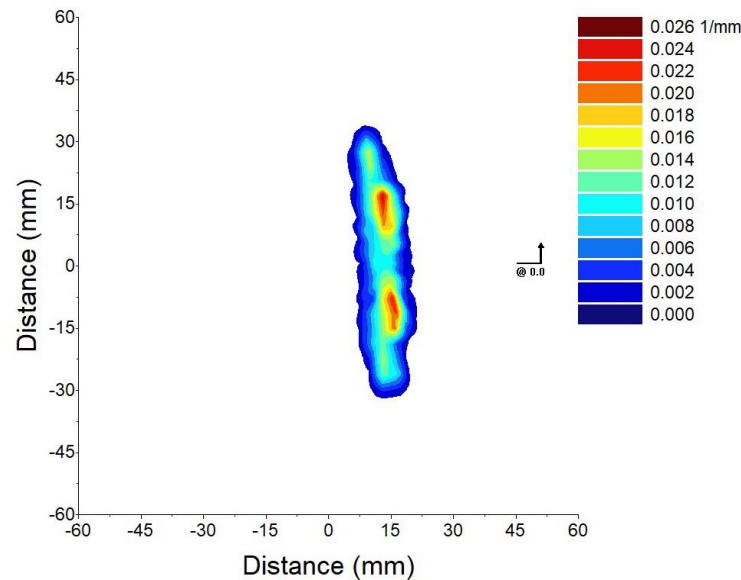

Figure 4. Sample contour plot from the windshield wiper nozzle A.

The contour map shows the elliptical pattern of a flat fan spray. In addition, there are two locations where the surface are density is high. The measurements were obtained at 40 mm below the exit plane. The colour bar shown along with the plot represents the local value of the total surface area density in units of mm-1. Blue colour represents shallow values for the local total surface area density and red represents high values.

The contour plot can be used to specify several parameters that characterize a spray. Only four parameters, namely, the mean spray angles, the radial distribution of surface areas, the angular distribution of surface areas, and the total surface area, are discussed in this study.

The first parameter that is discussed in some detail is the spray angles. For round sprays, the spray angle is calculated as 2*(tan-1 (R/X)). X is the distance of the measurement plane from the orifice's exit, and R is the radius that encloses a user-defined percentage of the total surface area. . For flat spray, the % at which the local extinction reaches a predetermined % of the peak extinction values is used. In this study, the 10% value is used for the spray angles. The variation of spray angle with the % of peak extinction value is shown in Fig. 5.

Several angles are generally of interest in the windshield wiper and the paint industry.. The first is the Aim angle. This is the angle from the plane of origin to the plane of the actual spray. The second is the major angle or also known as the Fan angle. This is the angle of the horizontal distribution of the spray seen from a top view. The third is the minor angle (also known as spray thickness). This is the thickness of the spray across the vertical axis when viewed from the top. The next is the roll angle or the angle by which the spray is rotated on the horizontal axis. The last is the Yaw Angle or the angle at which the spray is shifted along the horizontal axis. The patternator reports the major and minor angles and the X and Y location of the canter of the spray. This defines four of the five angles described above. Besides, the patternator performs an automatic rotation feature that allows the spray to be oriented along the horizontal axis by internally calculating the roll angle.

For this spray, 90% was chosen as the cut-off point for the spray. The major (fan) and minor (thickness) angles for Nozzle A are approximately 68.4 and 20.0 degrees, respectively. This enables the user to check the ellipticity of the spray.
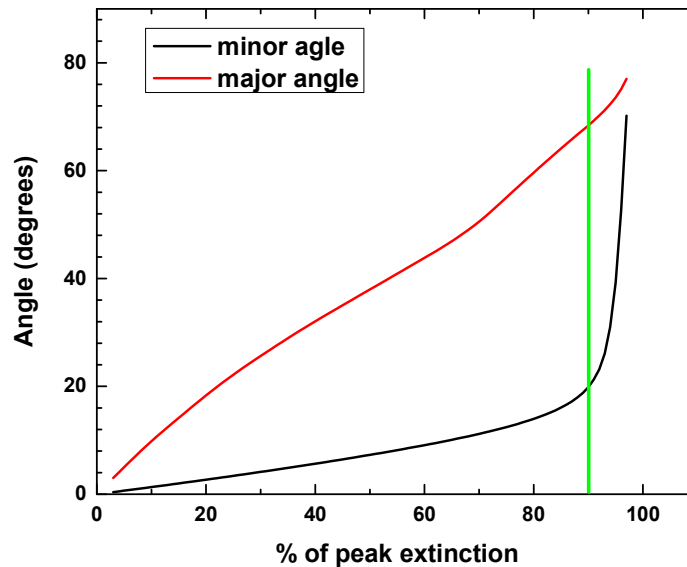

Figure 5. The variation in spray angle versus the % of peak extinction.

It can also be observed that the x location of the centre of the spray is not coincident with the centre of the nozzle. For the above nozzle, the (X,Y) location of the spray centre is given by the coordinates (13.16 mm, aim angle can be calculated as 13.24 mm. This corresponds to an aim angle of 18.31 degrees. From the Y- coordinate of the centre, the yaw angle can be calculated to be approximately 1.5 degrees. The roll angle provided by the system for Nozzle A is 85.24 degrees. The contour plot of surface area densities for Nozzle B is shown in Fig. 6.
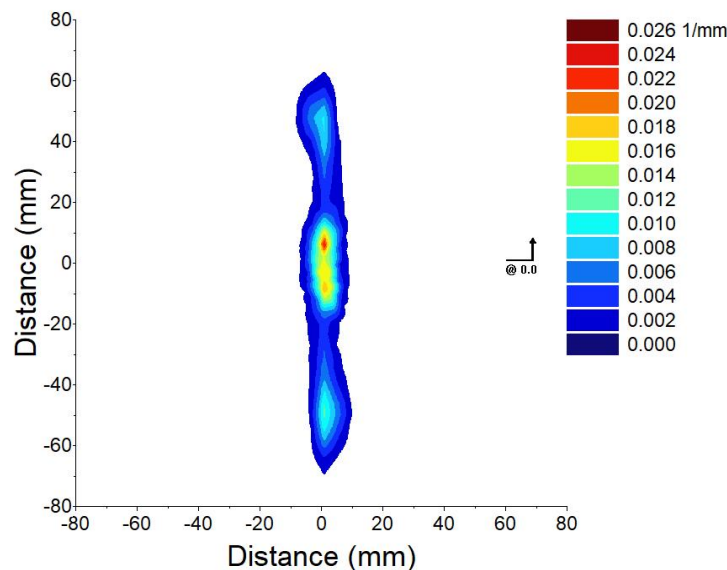

Figure 6. Sample contour plot from the windshield wiper nozzle B.

The major (fan) and minor (thickness) angles are approximately 108.7 and 28.9 degrees for nozzle B, respectively. The X and Y location of the centre of the spray is 1.02 and -2.66 mm. Therefore the distance of the spray centre is 2.84 mm. Therefore, the aim angle is

4.07 degrees. From the Y-co-ordinate, the Yaw angle is 3.80 degrees. The roll angle is approximately 89.0 degrees.

In addition to the five angles, the angular variation of the surface area density is usually examined to gauge the nozzle's symmetry. The angular variation in surface area density can be calculated from the contour maps as follows:

$$\Omega(\theta) = \int_0^R \xi(r,\theta)r\,dr \qquad (1)$$

where $\xi(r,\theta)$ is the drop surface area density shown in the contour maps in polar coordinates, r is the radial location from the centre of the nozzle, and θ is the azimuthal angle (the zero degrees location is shown in the contour maps). Once the angular profile of the surface area density, integrated along each angle is calculated, the profile is normalized to show the deviation of this profile from the mean value. The normalization is represented as:

$$\Omega_N = \frac{\Omega(\theta)}{\frac{360}{\int_0^{360} \Omega(\theta)\,d\theta}} *100 \qquad (2)$$

The normalized surface area densities for the two nozzles are shown in Fig. 7
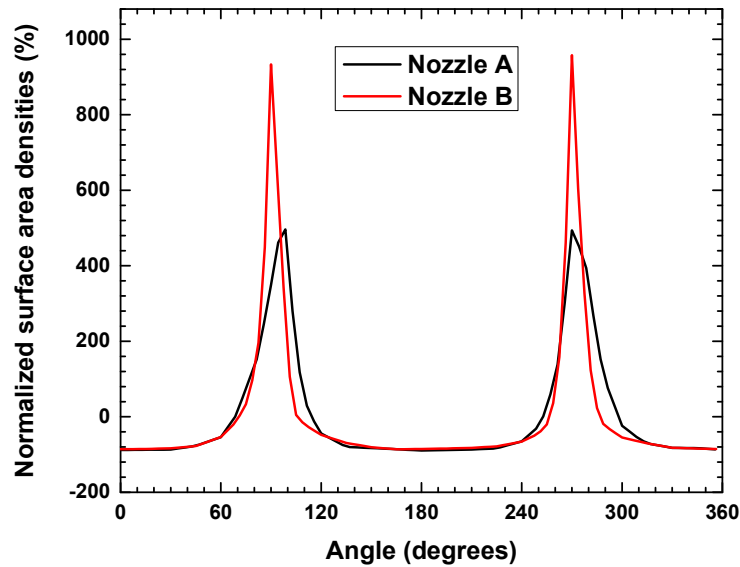

Figure 7. Normalized surface area density profiles for the windshield wiper nozzles.

The normalized profiles show the two peak locations corresponding to the major axis that is expected from a flat spray. The higher the value of the normalized variation in the angular profile, the more elongated or flatter is the spray. It can be seen that Nozzle B has a more elongated spray than Nozzle A. In addition, the symmetry is also higher for Nozzle B as compared to Nozzle A. Similar to the angular profile, radial profiles of surface area densities are typically presented for round sprays.

For flat sprays, the integrated surface area densities along the major axis are of more interest. The integrated surface area densities along the major axis can be represented as:

$$\Psi(x) = \frac{1}{K} \int_{-Y}^{+Y} \xi(x,y)\,dy \qquad (3)$$

where $\xi(r,\theta)$ is the contour of the local surface area densities in Cartesian coordinates, and K is the normalization constant, which in this case is the total surface area of the drops in the plane. Each value along the X-axis represents the fraction of the total surface area of the drops at that x location. Before the integrated surface area densities are calculated the contour maps are rotated so that the major axis of the spray is aligned to the X-axis. The integrated surface area densities along the major axis for the nozzles are shown in Fig. 8.
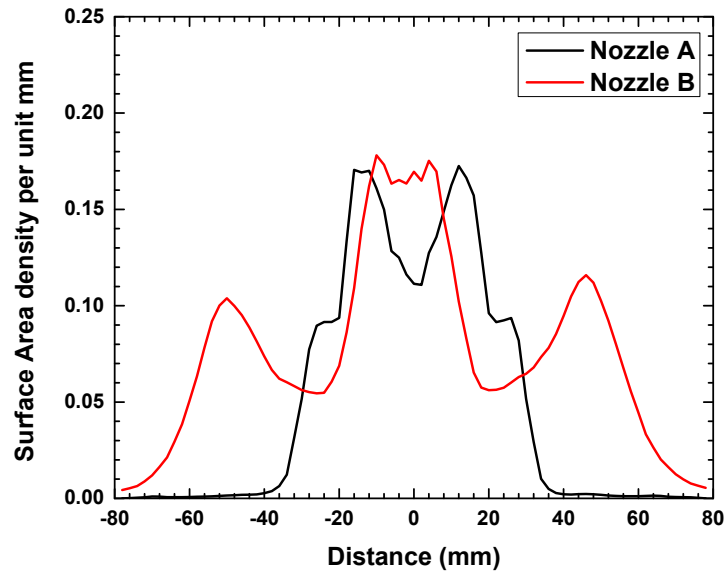

Figure 7. Surface area density profiles integrated along the major axis for the windshield wiper nozzles.

The last parameter that is reported in this study is the total surface area of the spray at the measurement plane. Physically, the entire surface area represents the cumulative surface area of all the drops within a 1mm height of the spray at the measurement location. This is one of the most critical parameters reported by the SETscan patternator. For a given flow rate, if there is a large number of small drops, the surface area will be higher than if there is a smaller number of large drops. For nozzle A, the total surface area of all the drops in a 1 mm thick plane is 7.03 mm^2 and, for nozzle B, the total surface area is 10.24 mm^2.

Conclusions

The definition of the five different spray angles that are used for flat fan sprays is also presented in this study. The conclusion of this study is that statistical extinction tomography is the ideal method for estimating the various spray angles in a flat spray that is representative of windshield wipers.

Acknowledgement

References

[1]   Sivathanu, Y. R., Lim, J., Wallace, B., and Seei, R., 2010, "A Comparison of Spray Angle Measurements using Optical and Mechanical Methods," Atomization and Sprays 20(1) pp. 85-92.

[2]   Hou, D., Zhang, H., Kalish, Y., Lee, C.F., and Cheng, W.L., 2009, "Adaptive PCCI Combustion Using Micro-Variable Circular-Orifice (MVCO) Fuel Injector—Key Enabling

Technologies for High Efficiency Clean Diesel Engines," SAE Pap. 2009-01-1528, SAE, Detroit, MI.

[3]   Xu, M. and Markle, L.E., 1998, "CFD-Aided Development of Spray for an Outwardly Opening Direct Injection Gasoline Injector," SAE Pap. 980493, SAE, Detroit, MI.

[4]   Tillmann, W., Vogli, E., and Krebs, B., 2008, "Influence of the Spray Angle on the Characteristics of Atmospheric Plasma Sprayed Hard Material Based Coatings," J. Thermal Spray Technol., vol. 17, pp. 948–955.

[5]   Im, K.-S., Lai, M.-C., Liu, Y., Sankagiri ,N., Loch, T., and Nivi, H., 2001, "Visualization and Measurement of Automotive Electrostatic Rotary-Bell Paint Spray Transfer Processes," J. Fluids Eng., vol. 123, pp. 237–245.

[6]   Silk, E. A., Kim, J., and Kiger, K., 2006, "Spray Cooling of Enhanced Surfaces: Impact of Structured Surface Geometry and Spray Axis Inclination," Int. J. Heat Mass Transfer, vol. 49, pp. 4910–4920.

[7]   Zhou, Q., Miller, P. C. H., Walklate, P. J., and Thomas, N. H., 1996, "Prediction of Spray Angle from Flat Fan Nozzles," J. Agric. Eng. Res., vol. 64, pp. 139–148.

[8]   Lefebvre, A. H., Atomization and Sprays, Hemisphere, New York, 1989.

[9]   Bush, S. G., and Collias, D. I., 1996, "Pattern Measurements in Fan Spray Atomizers with High Viscosity Fluids," Proceedings of ILASS Americas'96, San Francisco, CA.

[10] Ullom, M. J., and Sojka, P. E., 2001, "A Simple Optical Patternator for Evaluating Spray Symmetry," Rev. Sci. Instrum., vol. 72, pp. 2472–2477.

[11] Sellens, R., and Deljouravesh, R., 1997, "Non-orthogonal Optical Spray Pattern Analysis," Proceedings of ILASS Americas'97, Ottawa, ON.

[12] Smallwood, G. J., Gulder, O. L., and Snelling, D. R., 1994, "The Structure of the Dense Core Region in Transient Diesel Sprays," 25th International Symposium on Combustion, Pittsburgh, PA.

[13] Talley, D. G., Thamban, A. T. S., McDonell, V. G., and Samuelsen, G. S., 1995, "Laser Sheet Visualization of Spray Structure," Prog. Astron. Aeronaut., vol. 166, pp.113–141.

[14] Ruff, G. A., and Faeth, G. M., 1995, "Non-intrusive Measurement of the Structure of Dense Sprays," Prog. Astron. Aeronaut., vol. 166, pp. 263–296.

[15} Brown, C. T., McDonell, V. G., and Talley, D. G., 2002, "Accounting for Laser Extinction, Signal Attenuation, and Secondary Emission While Performing Optical Patternation in a Single Plane," Proceedings of ILASS Americas'02, Madison, WI.

[16] Hung, D. L. S., Harrington, D. L., Gandhi, A. H., Markle, L. E., Parrish, S. E., Shakal, J. S., Sayar, H., Cummings, D., and Kramer, J. L., 2008, "Gasoline Fuel Injector Spray Measurement and Characterization — A New SAE J2715 Recommended Practice," SAE Tech. Pap. 2008-01-1068, SAE, University of Wisconsin, Madison, WI.

[17] Berrocal, E., Sedarsky, D. L., Paciaroni, M. E., Meglinski, I. V., and Linne, M. A., 2007, "Laser Light Scattering in Turbid Media Part I: Experimental and Simulated Results for the Spatial Intensity Distribution," Opt. Express, vol. 10, pp. 10649–10665.

[18] Lim, J., Sivathanu, Y., Narayanan, V., and Chang, S., 2003, "Optical Patternation of a Water Spray using Statistical Extinction Tomography," Atomization and Sprays, vol. 13, pp. 27-43.

[19] Lim, J., and Sivathanu, Y., 2005, "Optical Patternation of a Multi-Orifice Spray Nozzle," Atomization and Sprays, vol. 15, pp. 687-698.

[20] VardiY., and Lee, D., 1993, "From Image Deblurring to Optimal Investments: Maximum Likelihood Solutions for Positive Linear Inverse Problems," J. R. Statist. Soc. B, vol. 55, pp. 569-612.